Polymer, 1991, Vol. 32, 181–190

Use of image analysis for the knowledge and control of polymer and Ziegler–Natta catalyst granulometry

J. C. Bailly
BP Chemicals S.N.C., Centre de Recherche, BP No 6, 13117 Lavera, France

and R. Hagege
Institut Textile de France, 280 Avenue Aristide Briand, 92223 Bagneux Cedex, France
(Received 6 March 1989; revised 4 October 1989; accepted 16 November 1989)

A procedure for the quantitative assessment of granulometry of catalyst and polymer particles by SEM image analysis is described. The main advantages of this method, as compared to existing techniques, are: better reliability; reproducibility; ease of manipulation. Application of the procedure to Ziegler–Natta type catalysts of 2nd and 3rd generations and to polyolefins obtained from these catalysts, shows that there is a close correlation between the shape of catalyst particles (close to spherical) and that of corresponding polymer granules whatever the productivity of the chemical reaction.

(Keywords: SEM; polyolefins; polypropylene; granulometry; Ziegler–Natta catalysts; image analysis; productivity)

AIM OF THE STUDY

Correlations between the granulometry of solid Ziegler–Natta catalysts and that of olefinic polymers prepared therefrom are the subject of major studies by polymer producers and physicochemists. The same is true as far as the laws governing the granulometric evolution of particles during the process are concerned[1].

In the course of industrial polymerization of olefins with Ziegler–Natta type catalysts, the evolution in size of the growing particles must be controlled. Indeed, this evolution has a significant influence on the stability of the 'stirring' regime, whatever the dispersion method used (suspension within a hydrocarbon liquid or dry phase, e.g. fluidized bed). Another reason for the usefulness of an adequate control of the final polymer granulometry is the following: there is a strong correlation between the granulometry and the so-called post-polymerization steps, i.e. transport and storage of powders, blending with additives, feeding of polyolefin processing machines, etc. Such considerations led us to try to improve the existing techniques for granulometric measurements[2,3].

The present study is concerned with the morphological characterization and the granulometric control of granules of Ziegler–Natta catalysts and of the polymers obtained therefrom. It was performed by means of an image analyser interfaced with a scanning electron microscope (SEM). The method allows the visual observation of particles through electron micrographs (surface appearance, porosity, shape of particles, etc.). It also allows the statistical determination of dimensions of those particles from the numerical processing of micrographs. This method considerably improves on the ones currently used. Let us quote some of them:

(i) Dry-phase techniques, e.g. sifting by means of a series of sieves and a sieve stirrer. Such a method is generally suited to particles of sufficient size, e.g. larger than 100 μm, and which show a weak electrostatic behaviour, a fairly flat granulometry, and which can be examined in air. In fact, such a method cannot be used for catalyst particles and does not allow morphological observation of particles.

(ii) Solution-phase techniques, e.g. by potentiometry using a Coulter counter apparatus from Coultronics Ltd[4,5]. These methods are not easy to use for catalyst particles and do not allow morphological observations. Moreover, particles are assumed to have a spherical shape as far as granulometric measurements are concerned.

(iii) Laser diffraction techniques, e.g the so-called Malvern apparatus[6]. In this, particles are assumed to have a spherical shape and cannot be studied morphologically. Although this method could be used, in principle, under an inert atmosphere, it proves fairly difficult to use effectively, especially in the case of catalysts.

(iv) As far as image analysis using Optomax-type[7] systems is concerned, even interfaced with an electron microscope, the software available for granulometry is not powerful. One has to count particle by particle, and it is impossible to take into account particles in contact with one another.

The method proposed below permits the resolution of many of the above-mentioned problems. It is an image processing and analysis technique based on direct SEM examination. In addition to the depth of analysis provided by such an instrument, the method involves a set of specially developed software aimed at optimizing the accuracy of granulometric measurements. Analysed particles can have dimensions ranging from 10^{-2} μm to a few millimetres. Sample preparation can be performed

0032-3861/91/010181-10

either in air with no special precautions (for polymers) or under a controlled atmosphere (for catalysts). Moreover, complete separation between individual particles is not required. The study was concerned with catalyst and polymer particles with a more or less isodiametric shape.

INSTRUMENTS AND METHODS

SEM and image enhancing system

SEM is used mainly on account of its depth of focus, and because samples are examined in air-free conditions (under a low pressure of the order of 10^{-5} Torr). This second aspect is especially interesting for the study of oxidation-sensitive materials, the morphology of which is oxidation labile, e.g. Ziegler–Natta catalysts. For such objects, the transfer into the examination chamber of the SEM was performed through a specially designed system under N_2 atmosphere.

SEM images of polymers are generally fairly noisy and lack contrast. The use of a well-fitted processing system is frequently recommended. In the present work, a 'Crystal' device[8] was used. This comprises a scanning generator, which can be substituted for the microscope's internal scanning generator and allows us to acquire the signal delivered by either of the instrument's detectors (here, only the secondary electron detector was concerned) and to process it in 'real time'.

The main functions available on 'Crystal' are:

(a) contrast–brilliance function (on the digital image),
(b) time averaging, and
(c) spatial averaging.

The images thus enhanced are subsequently sent to the image analyser, which performs additional processing and mathematical computations. Results and reports are presented through a typewriter. One may also send back on the SEM photographic screen modified images (e.g. binary images arising from thresholding) from the image analyser. These images can thus be printed by the same system used for 'local' SEM work.

Diagram of the system

This is shown in *Figure 1*[9]. Cable (I) enables us to send the images given by SEM to the image analyser, while the mouse (S) commands the (generally remote) microcomputer (PC), through the cable (0). Thus, the SEM images, which were previously digitized by 'Crystal', can be stored on the computer disc (they are generally analysed in a separate session). Before storing, these digital images can be enhanced by using the 'extended command box' (B). Alternatively, this enhancement can be done on stored images, just before processing: in that case, (B) is carried close to the PC. Special software was developed in order to store and 'label' these images ready for analysis. This software comprises a security auto-test to ensure that the storage is correct, before moving the sample to a new area of interest under the SEM. This test is especially interesting for samples that are not reusable after having been removed from the microscope.

Cable (II) allows us to send back towards 'Crystal' images stored in the PC, or alternatively images from another source, e.g. an external camera, fitted with a 'macro' objective, shown on the upper right of the figure, with its transfer cable (III) to the analyser. The transfer is usually performed between monitors, because 'Crystal' is mainly dedicated to the SEM.

Image processing and analysing

The system used in the present work is based on an image processor called '151 series'[10], with a host IBM PC AT3 in which the 'Visilog' software[11] was implemented. Visilog comprises a number of algorithms, in particular 'Mathematical Morphology'. For the present work, one has to deal with a granulometric application. The images are sometimes of low contrast, despite the use of 'Crystal', so a combination of automatic sequences and manual steps proved useful. The main steps of processing are the following:

(a) thresholding and binarization;
(b) removing of noise ('particles' of a few pixels);
(c) first separation of particles, by background skeletization;
(d) labelling of remaining aggregates of particles;
(e) second separation (background skeletization);
(f) image regeneration with 'fully' separated particles.

Figure 2 shows some sequential aspects observed on the final screen (after feedback to the SEM), in a simple case, in which only one separation is sufficient:

(1) image 1 shows the initial electron image, allowing all the morphological examination;
(2) image 2 shows the binary image extracted from image 1 through thresholding;
(3) image 3 is the binary skeleton of the complement of image 2;
(4) image 4 is the logical difference between images 2 and 3, i.e. image 2 with fully separated particles.

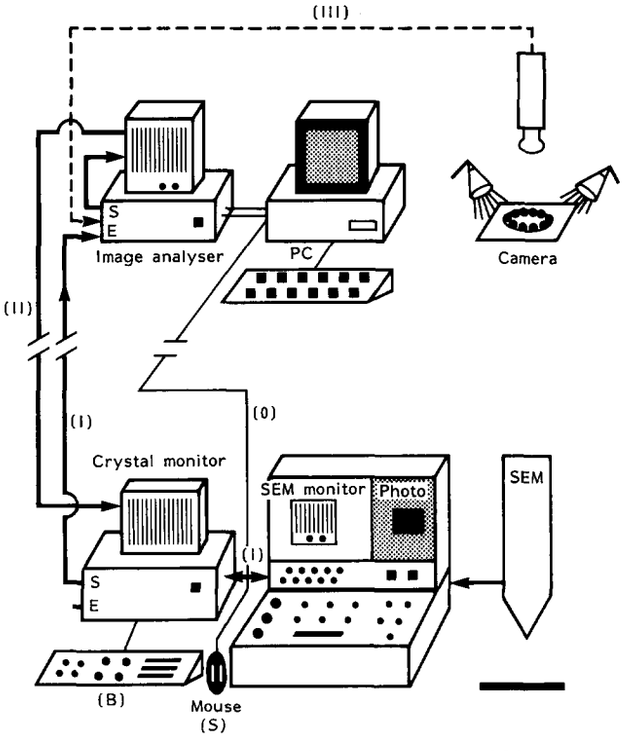

Figure 1 Diagram of the system for acquisition of SEM images

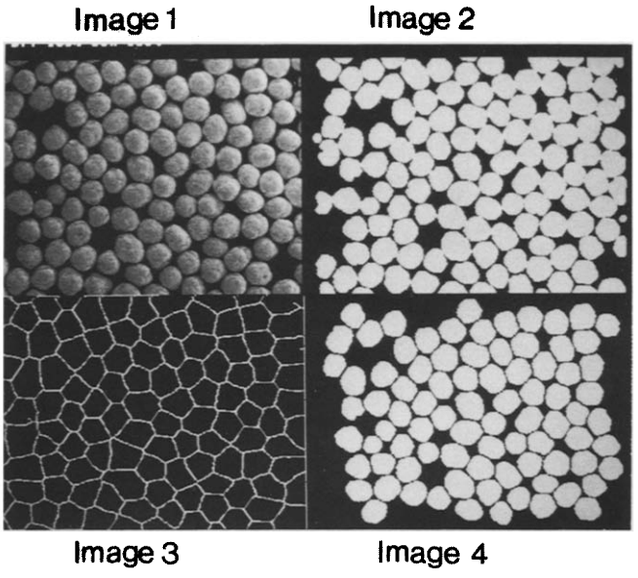

Figure 2 Steps for image processing

At this stage, individual measurements of relevant parameters are performed: the most useful ones are area, equivalent diameter, perimeter and, finally, 'circularity index' (i.e. a non-dimensional number c related to the ratio between square of perimeter P and area S; $c=P^2/4\pi S$). These parameters are finally presented in the form of mean values with corresponding standard deviations: one generally accumulates several images in order to get a statistical average of several tens of distinct particles (taking into account the fact that some data are cancelled out because of, e.g. an inadequate separation between particles). For illustration purposes, experimental values corresponding to ten particles of one sample examined in the present study are presented in *Table 1*.

Sample preparation

The technique is close to that generally used in SEM work. A certain number of particles are deposited on a metallic sample holder (a small 1 cm diameter cylindrical block). The whole preparation is metal-coated prior to SEM introduction. Polymeric particles must be stuck on the sample holder by means of double-sided adhesive tape, whereas catalyst particles may be merely deposited on the block without any glue or metal-coating. On the other hand, in the latter case, one must use a glove-box, with an inert atmosphere in order to prevent any contamination by moist air. In that situation, the transfer to the SEM examination chamber must likewise be performed under inert atmosphere. One generally uses a suspension of the catalyst particles in a hydrocarbon liquid, under an inert atmosphere. Once this suspension is homogeneous, a drop of it is taken and deposited on the sample holder. Then the hydrocarbon liquid is evaporated in the nitrogen box. Such sample preparation will be said to be of good quality if catalyst particles are arranged into a monolayer on the surface of the sample holder.

In the case of polymeric samples that can be manipulated in air, care should be taken with the monolayer distribution of the particles. One should not try to separate them systematically from one another, which is a very difficult task, on account of the tendency to agglomeration caused by electrostatic forces.

Table 1 Examples of granulometry of one of the images of sample 3 of experimental series 1 (see *Table 2*): magnification ×480 (0.823958 μm/pixel)

	Surface (μm)	Perimeter	Diameter	Circularity
1	571.64	102.17	26.98	1.45
2	589.29	98.88	27.39	1.32
3	661.26	108.76	29.02	1.42
4	537.02	93.93	26.15	1.31
5	561.46	97.23	26.74	1.34
6	559.42	98.88	26.69	1.39
7	547.88	97.23	26.41	1.37
8	494.24	92.28	25.09	1.37
9	721.68	117.00	30.31	1.51
10	587.93	102.17	27.36	1.41

Figure 3 shows various qualities of sample preparations for image analysis:

(i) micrograph *3a* is the case of an unprocessable multilayer;

(ii) on micrograph *3b*, one can see some particles in contact (upper left corner)—such a case must be processed manually;

(iii) micrographs *3c* and *3d* represent the ideal case—processing will be fully automatic.

The micrographs in *Figures 3a, 3b* and *3c* correspond to catalyst preparations obtained under nitrogen atmosphere (sample 1 of the experimental series no. 3, *Table 2* below); that in *Figure 3d* represents one image from polymer particles of samples 12 from experimental series no. 1 (*Table 2*).

Each image, according to the particle size and the magnification used for SEM, comprises particles between about 20 and 60 in number.

THE SAMPLES EXAMINED

Catalysts

Olefinic polymerization catalysts of second and third generation were considered. Second-generation catalysts are based on $TiCl_3$ and their preparation was similar to the one described in French patents[12–14]. As far as third-generation catalysts are concerned, they are also based on titanium. They are so-called 'superactive' catalysts formed from an inorganic support. They were prepared according the description given in European patents[15–17]. All these catalysts are well suited for olefin polymerization, as well as interolefin copolymerization.

Polymers

Only polypropylene granules produced in a batch polymerization process, in suspension in a hydrocarbon liquid, were considered. The residence time of each growing polymer particle in the reaction medium may thus be considered identical. Various advancement ratios* were achieved, by modifying the operating conditions. The samples obtained are listed below:

* The advancement ratio is often referred to as the catalyst productivity; we use units of grams of polymer per millimole of titanium

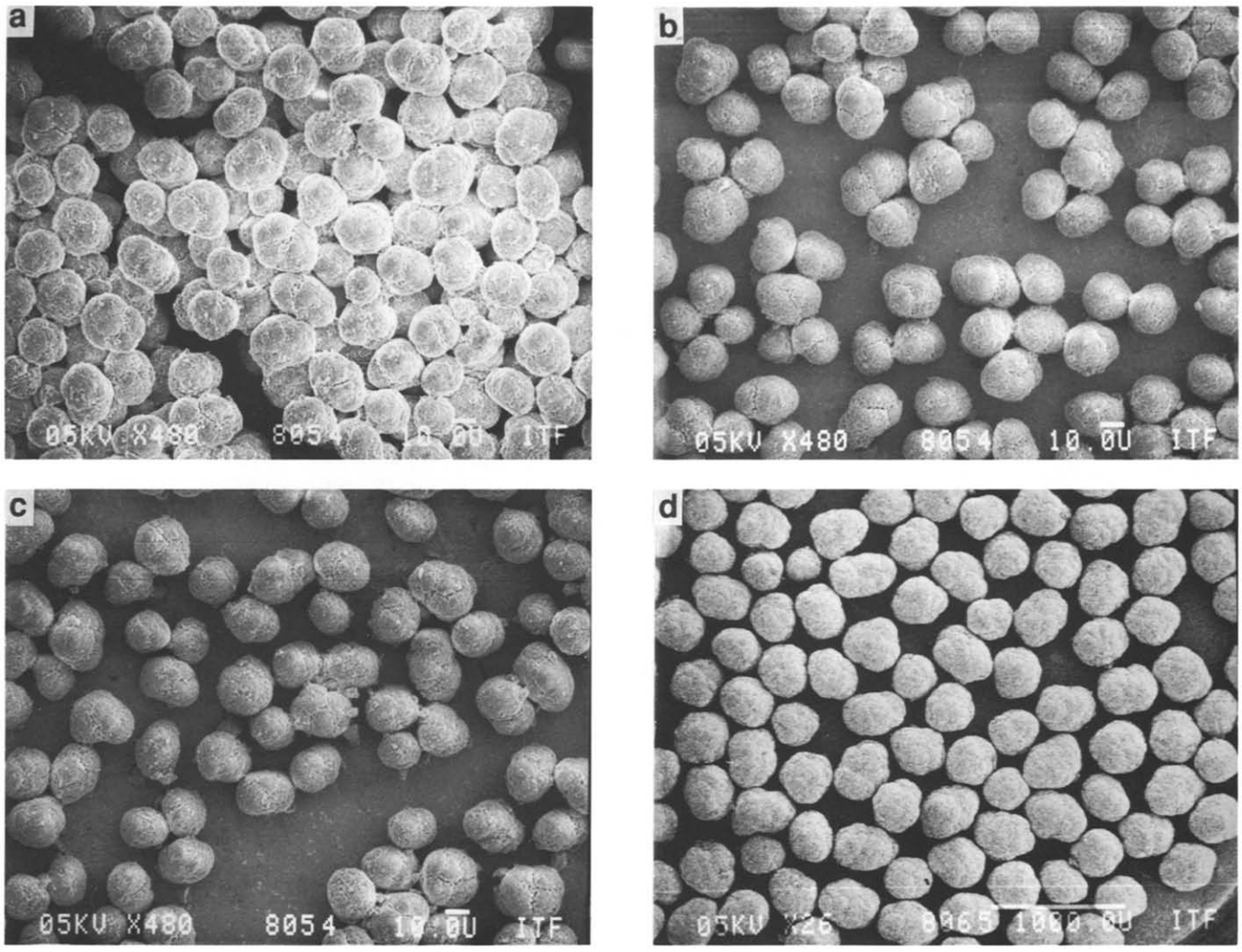

Figure 3 Some typical micrographs for image analysis: (a) multilayer; (b) a few aggregates; (c) a suitable image for catalyst; (d) a suitable image for polymer

(a) particles at very low advancement ratio, ~1 g polypropylene per millimole titanium (so-called 'coated catalyst');

(b) particles at a low advancement ratio, of the order of a few tens of grams polypropylene per millimole Ti (so-called 'prepolymer');

(c) particles at a much higher advancement ratio, of the order of 1 kg polymer per millimole Ti as far as second-generation catalysts are concerned, and of the order of some tens of kilograms per millimole Ti, as far as third-generation superactive catalysts are concerned—these particles are polymers similar to those produced in industrial polymerizations.

Evaluation of productivities for polymers

In the case of 'coated catalysts', this measurement is performed by physicochemical methods, like colorimetry or atomic absorption. Titanium content in a known weight of coated catalyst is measured by either method, after total solubilization of the titanium compound.

As far as prepolymers at an advancement ratio higher than 25 g/mmol Ti (i.e. 2000 ppm Ti) are concerned, a measurement technique for titanium by X-ray fluorescence on a dry melt-processed polymer pellet was used. The same is true in the case of polymers with an advancement ratio lower than 10 kg/mmol Ti (i.e. 5 ppm Ti). This X-ray fluorescence method gives results that are in very good agreement with the figures deduced from the amount of titanium introduced at the beginning of the process, and the amount of polymer produced. For higher advancement ratios (more than 10 kg/mmol Ti) the X-ray fluorescence method lacks precision. In such a situation, advancement ratio measurement was based solely on determination of the weight of polymer synthesized.

RESULTS

In *Table 2* experimental results arising from image analysis (diameter, circularity) are shown for the five experimental series considered in the present study. The first experimental series is concerned with a second-generation catalyst, while the other series are related to four distinct third-generation catalysts, with four different sizes. Standard deviation σ of the sample and Student's coefficient $s=\sigma/\sqrt{n}$ (the latter allowing for the calculation of the confidence interval for the mean) are indicated.

Table 3 shows results of mean diameters (from *Table 2*) and of advancement ratios, in logarithmic form.

Figure 4 represents the regression line, together with experimental points, for the second-generation catalyst (experimental series no. 1, in *Table 3*). Characteristic data of the regression are indicated in the caption.

Table 2 Experimental values of diameters, productivities and circularities of catalyst and polymer particles

Exp. ser.		Catalyst 1	Polymers 2	3	4	5	6	7	8	9	10	11	12
1	n	175	87	155	96	195	136	157	210	231	307	299	354
	d (μm)	12.7	20.7	25.8	32.6	42.9	53.0	62.9	106	147.5	231	264	343
	σ	1.3	2.4	2.4	3.5	4.9	5.8	6.1	14.9	17.0	26.7	33.5	36
	s	0.1	0.3	0.2	0.4	0.35	0.5	0.5	1.0	1.1	1.5	1.9	1.9
	c	1.30	1.41	1.40	1.40	1.34	1.43	1.38	1.38	1.37	1.29	1.28	1.25
	σ	0.07	0.28	0.09	0.16	0.12	0.09	0.11	0.18	0.08	0.08	0.07	0.06
2	n	126	113	122	92	73	94	111	101				
	d	16.4	52.2	67.7	76	183.4	196	432	455				
	σ	1.8	7.3	8.8	9.1	20.2	21.5	47.5	55				
	s	0.16	0.7	0.8	0.95	2.4	2.3	4.5	5.5				
	c	1.27	1.07	1.02	1.07	1.03	1	1.07	1.01				
	σ	0.10	0.01	0.01	0.03	0.01	0.02	0.01	0.01				
3	n	181	353	291	281	229	230	314	341				
	d	18.5	74.8	87.5	96.5	392.9	409.3	511.7	522.1				
	σ	2.6	13.3	15.1	14.9	56.4	51.9	67.0	59.1				
	s	0.2	0.7	0.9	0.9	3.7	3.4	3.8	3.2				
	c	1.33	1.01	1.07	1.05	1.06	1.13	1.13	1.04				
	σ	0.08	0.20	0.29	0.08	0.26	0.37	0.36	0.55				
4	n	148	102	149	458	495	457	500	155	154	143	137	
	d	20.6	29.3	35.9	67.1	86.2	99	108.3	508	548	549	566	
	σ	2.5	5.4	5.5	10.5	12.6	13.7	14.3	62.3	60.4	63	71	
	s	0.2	0.5	0.45	0.5	0.6	0.6	0.6	5.0	5.0	5.3	6.1	
	c	1.36	1.50	1.47	1.02	1.02	1.03	1.03	1.10	1.08	1.13	1.11	
	σ	0.08	1.24	0.72	0.06	0.06	0.06	0.06	0.10	0.13	0.13	0.08	
5	n	125	197	217	237	135	166	241	163	155	110	112	91
	d	24.3	33.5	34.8	106.6	129.2	133.2	431.6	593.6	594.6	661.9	674.7	676.0
	σ	2.7	3.7	4.5	15.9	18.2	23.5	81.2	90.8	61.7	83	88.6	94.3
	s	0.2	0.3	0.3	1.0	1.6	1.8	5.2	7.1	4.9	7.9	8.4	9.9
	c	1.41	1.40	1.42	1.02	1.03	1.16	1.09	1.23	1.09	1.07	1.19	1.07
	σ	0.09	0.25	0.20	0.13	0.04	0.35	0.31	0.48	0.06	0.06	0.38	0.06

n = number of particles analysed per sample
d = mean diameter of the n particles of sample
c = mean circularity of the n particles of sample

Table 3 Logarithms of the experimental values of productivities and mean diameters of catalyst and polymer particles

Exp. ser.		Catalyst 1	Polymers 2	3	4	5	6	7	8	9	10	11	12
1	X	1.104	1.316	1.412	1.513	1.632	1.724	1.799	2.025	2.169	2.364	2.421	2.555
	Y		−0.347	−0.097	0.176	0.653	0.881	1.124	1.778	2.155	2.851	3.000	3.301
2	X	1.215	1.718	1.831	1.881	2.263	2.292	2.635	2.658				
	Y		1.681	2.079	2.204	3.255	3.477	4.398	4.489				
3	X	1.267	1.874	1.942	1.985	2.594	2.612	2.709	2.718				
	Y		2.097	2.230	2.389	4.243	4.279	4.556	4.568				
4	X	1.314	1.467	1.555	1.827	1.936	1.996	2.035	2.706	2.739	2.740	2.753	
	Y		0.643	0.929	1.740	2.041	2.250	2.352	4.279	4.382	4.398	4.477	
5	X	1.386	1.530	1.542	2.028	2.111	2.121	2.635	2.773	2.774	2.821	2.829	2.830
	Y		0.602	0.707	2.164	2.380	2.405	4.041	4.292	4.334	4.398	4.433	4.484

$X = \log[d\ (\mu m)]$ and $Y = \log(\text{productivity in g/mmol Ti})$

Figure 5 represents, without experimental points, the four regression lines related to all four third-generation catalysts in the present study (i.e. experimental series 2, 3, 4 and 5 in *Table 3*). Characteristic data of those four regressions are indicated in the caption.

On *Figures 6* and *7* some micrographs of second- and third-generation catalyst particles and of corresponding polymer particles are shown, for illustration purposes. All these SEM micrographs were taken during the course of the statistical determination of dimensions of particles.

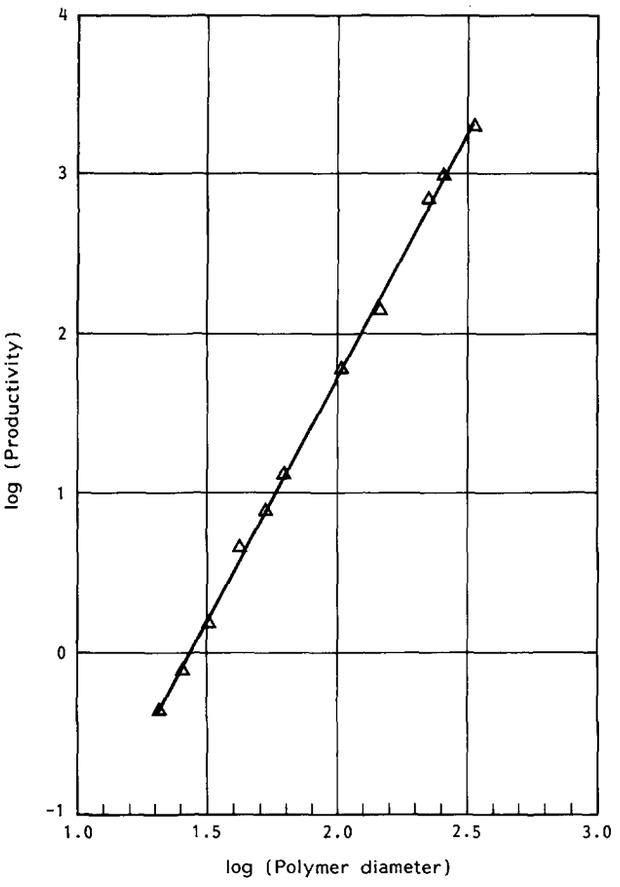

Figure 4 Regression line and experimental points for second-generation catalyst (series 1), showing excellent correlation between productivity and diameter of polymers: slope 3.027 ($\sigma = 0.031$), first ordinate -4.347 ($\sigma = 0.059$)

Such micrographs allow visual checking of surface morphology, porosity and shape. On *Figure 6a*, second-generation catalyst particles with a mean diameter of 12.7 μm are observed, while on *Figure 6b* one sees a polypropylene particle produced with this catalyst. On *Figure 7a*, third-generation catalyst particles with a mean diameter of 20.6 μm are observed, while a polypropylene particle produced with this catalyst is seen on *Figure 7b*. On *Figures 7c* and *7d*, micrographs at increasing magnifications of one particle from *Figure 7b*, with its surface morphology, are presented.

DISCUSSION

General considerations about particle size and shape measurement

Table 4 allows comparison of the variability of different data related to the whole set of samples from the five experimental series. A striking feature is the fact that the coefficient of variation for diameters (σ/d) remains within a relatively narrow interval (i.e. between 9.3% and 18.8%) whatever the advancement ratio of polymers and the origin of catalysts. In fact, as shown by a closer examination, this interval is even narrower if one considers only one experimental series. For instance, in the case of series no. 1 (second-generation catalyst), the interval is from 9.3% to 14.1%. As far as series no. 2 is concerned (third-generation catalyst, but only eight experimental values) it is from 11% to 14%. Such observations underline again[18] the fact that the granulometric distribution of the catalyst may be deduced from that of the polymer prepared therefrom. Moreover, the granulometric distribution of second- and third-generation catalysts examined in the present work was directly estimated and proved fairly narrow: coefficient of variation $\sim 12\%$. In addition, the present method gave a very good estimation of mean diameters: values of $s/\bar{d}$ ratio lie between 0.6% and 1.7%.

The above correlation coefficients are highly significant, on a statistical basis. Indeed, for the numbers of degrees of freedom (i.e. the number of pairs of values minus 2) of 10 and 37, respectively, for second- and third-generation catalysts, the significance limit—at a probability threshold of 0.99—is 0.708 and 0.410, whereas the corresponding experimental coefficients are 0.824 and 0.740. With a total of only 150 particles examined (corresponding to a maximum of six images processed), a precision of $\sim 1\%$ is obtained, as far as mean diameters are concerned. Such a method is thus able to give useful information on mean dimensions and on the 'true' dispersion of the populations of particles from which samples of catalysts or polymers were taken.

As far as shape is concerned, no circularity above 1.50 was observed. We recall that a square shape corresponds to a circularity of 1.27, and a rectangle with an aspect ratio of 3 gives a circularity of 1.70. If one takes into account that the images studied are 2D projections of 3D objects, one may conclude that the particles studied generally have a fairly good isodiametric character. In the case of the five catalysts studied, circularity does not significantly change between them, and is near 1.30. Moreover, circularity is only marginally altered during polymerization, and without any apparent correlation with the advancement ratio. The last observation confirms that there is a replication relationship between catalyst particles and polymer particles, whatever the advancement ratio.

Relationship between polymer particle dimensions and corresponding advancement ratio

Such a relationship has already been proposed in the course of previous general studies on polyolefins, using different measurement techniques[19–22].

From *Figures 4* and *5*, one sees that there is a

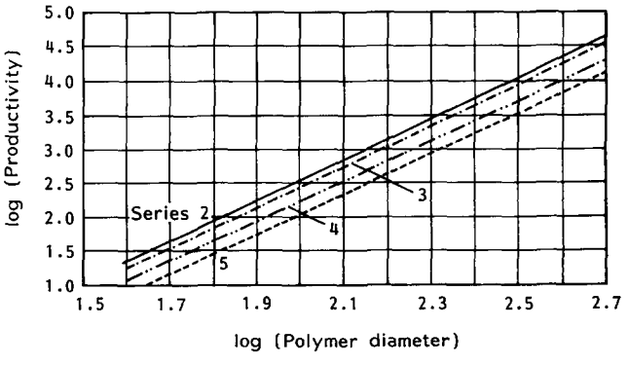

Figure 5 The four regression lines for third-generation catalysts. Series 2: slope 2.944 ($\sigma = 0.052$), first ordinate -1.343 ($\sigma = 0.115$), $r = 0.9992$, $n = 7$. Series 3: slope 2.992 ($\sigma = 0.028$), first ordinate -3.544 ($\sigma = 0.067$), $r = 0.9998$, $n = 7$. Series 4: slope 2.933 ($\sigma = 0.015$), first ordinate -3.362 ($\sigma = 0.034$), $r = 0.9999$, $n = 10$. Series 5: slope 2.943 ($\sigma = 0.035$), first ordinate -3.841 ($\sigma = 0.084$), $r = 0.9994$, $n = 11$

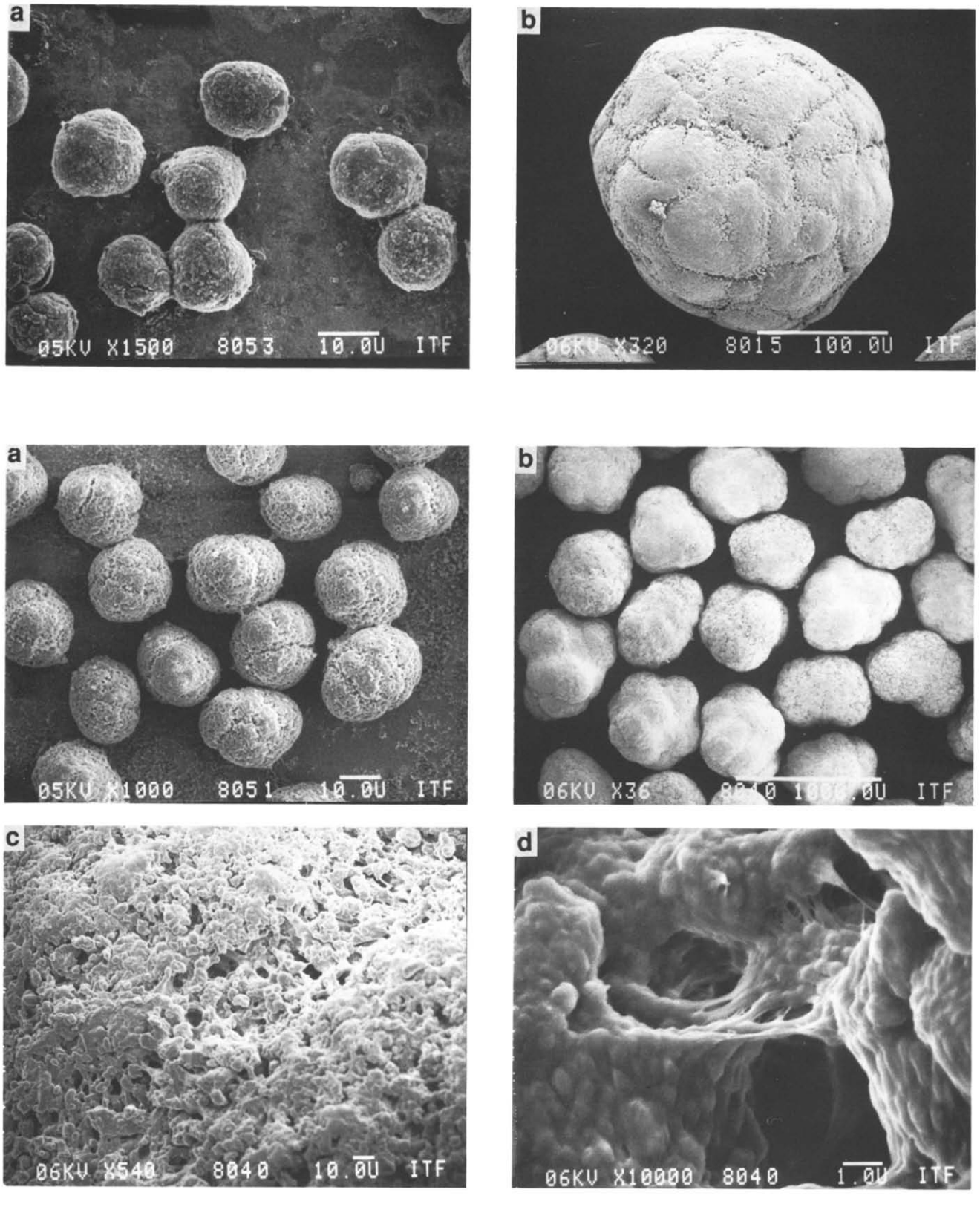

Figure 7 (a) Particles of third-generation catalyst. (b) Propylene particles from third-generation catalyst. (c), (d) As (b), showing surface aspects at increasing magnifications

very good linear correlation between the logarithm of advancement ratio and the logarithm of the corresponding mean diameter of polymer particles, whatever the catalyst considered (second or third generation).

The five correlation coefficients are statistically highly significant. Indeed, for a number of degrees of freedom which is always at least 5 (the number of pairs of values minus 2), the significance limit, for a probability threshold of 0.99, is seen to be 0.8745, whereas experimental coefficients are all above 0.999.

As far as the slopes of regression lines (see *Figures 4* and *5*) are concerned, taking into account the dispersity

Table 4 Percentage variability of diameters and circularities of catalyst and polymer particles

		Catalyst	Polymers										
		1	2	3	4	5	6	7	8	9	10	11	12	Range (%)
1	σ/d	10.2	11.6	9.3	10.7	11.4	10.9	9.7	14.1	11.5	11.3	12.7	10.5	9.3–14.1
	s/d	0.8	1.4	0.8	1.2	0.8	0.9	0.8	0.9	0.7	0.6	0.7	0.6	0.6– 1.4
	σ/c	5.4	19.9	6.4	11.4	9.0	6.3	8.0	13.0	5.8	6.2	5.5	4.8	4.8–19.9
2	σ/d	11.0	14.0	13.0	12.0	11.0	11.0	11.0	12.1					11.0–14.0
	s/d	1.0	1.3	1.2	1.3	1.3	1.2	1.0	1.2					1.0– 1.3
	σ/c	7.9	0.9	1.0	2.8	1.0	1.8	0.9	1.0					0.9– 7.9
3	σ/d	14.1	17.8	17.2	15.4	14.4	12.7	13.1	11.3					11.3–17.8
	s/d	1.1	0.9	1.0	0.9	0.9	0.8	0.7	0.6					0.6– 1.1
	σ/c	6.0	19.8	27.1	7.6	23.5	32.7	31.9	5.8					5.8–32.7
4	σ/d	12.1	18.4	15.3	15.6	14.6	13.8	13.2	12.3	11.0	11.5	12.5		11.0–18.4
	s/d	1.0	1.7	1.3	0.7	0.7	0.6	0.6	1.0	0.9	1.0	1.1		0.6– 1.7
	σ/c	5.9	83.0	49.0	5.9	5.9	5.8	5.8	9.1	10.2	11.5	7.2		5.8–83.0
5	σ/d	11.1	10.9	12.9	14.9	14.1	17.6	18.8	15.3	10.4	12.5	13.1	13.9	10.4–18.8
	s/d	0.8	0.9	0.9	0.9	1.1	1.5	1.2	1.2	0.8	1.2	1.2	1.5	0.8– 1.5
	σ/c	6.4	17.9	14.1	12.7	30.2	3.9	28.4	39.0	5.5	5.6	31.9	5.6	3.9–39.0

of results, all five are substantially equal to 3: the lines are thus parallel, as can be seen on *Figure 5*.

One may deduce from the above considerations that the following equation describes the growing behaviour of polymer granules:

$$\log(\text{advancement ratio}) = 3 \log \bar{d}_p + b$$

or

$$\text{advancement ratio} = K\bar{d}_p^3 \qquad (1)$$

with $b = \log K$ and $\bar{d}_p$ = mean diameter of polymer particles.

For each experimental series, there is a corresponding b value and consequently a corresponding K value (first ordinate $= b = \log K$). Each catalyst may then be characterized by the latter. It is clearly seen that the second-generation catalyst (experimental series no. 1) has a K value very significantly different (by a factor of 10) from K values of third-generation catalysts (experimental series 2–5). If one compares the third-generation catalysts between themselves, one finds b values only slightly different. This is a consequence of the small differences between the mean diameters of the catalysts studied, as discussed in the next section.

Relationship between K *coefficient and diameter of corresponding catalyst*

Here only third-generation catalysts ('superactive' catalysts) are examined, because they are currently of major interest to polymer producers[23].

Figure 8 shows the results of the correlation between $b = \log K$ values for experimental series 2–5, and values of the logarithms of mean diameters of corresponding catalysts. A good correlation is observed, since the correlation coefficient obtained, 0.993, corresponds to the probability threshold 0.99, for number of degrees of freedom equal to 2 (four pairs minus 2).

The value obtained for the slope ($a = 2.8$) is much less precise than those previously found in the course of the study of polymer advancement ratios. The standard deviation on this slope is indeed 0.232. Such poor precision can be explained, on the one hand, on the basis

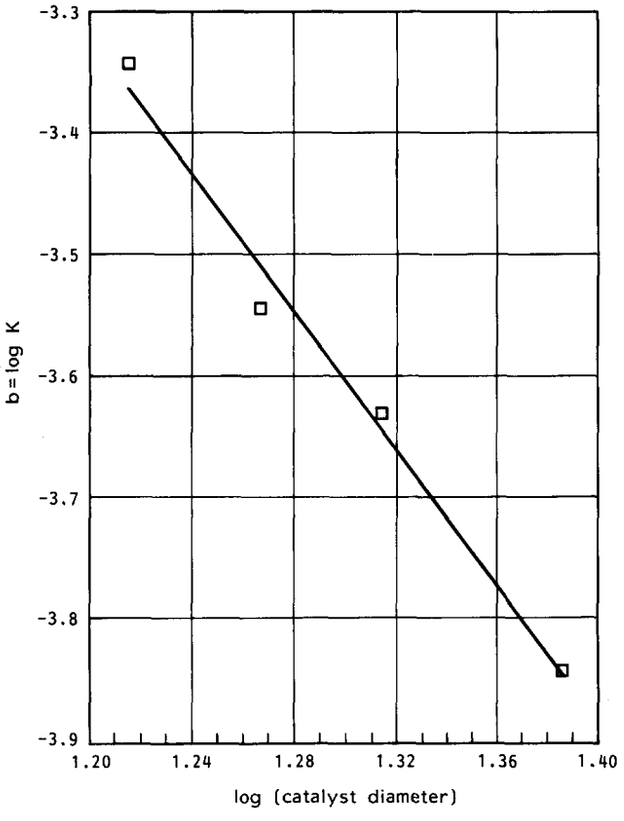

Figure 8 Correlation between $b = \log K$ and catalyst diameter for third-generation catalysts: slope -2.824 ($\sigma = 0.232$), first ordinate $+0.068$ ($\sigma = 0.301$), $r = 0.9993$

of the relative lack of precision on the individual b values, and, on the other hand, by the fact that the interval of variation of the diameters of the catalysts studied is only from 16.4 to 24.3 μm whereas the interval was from ~ 30 to $\sim 700\,\mu$m in the case of polymers.

The following equation is obtained:

$$\log K = -2.8 \log \bar{d}_c + \log k$$

or

$$K = k/\bar{d}_c^{2.8} \quad (2)$$

where $\bar{d}_c$ is the catalyst particle mean diameter. Combining equations (1) and (2), one gets for the advancement ratio the following relationship:

$$\text{advancement ratio} = k(\bar{d}_p^3/\bar{d}_c^{2.8}) \quad (3)$$

Theoretical derivation of advancement ratio

The following calculation allows us to obtain an equation with a similar form to equation (3). Let P_p be the mass of polymer obtained at a given time (expressed in grams). If P_c is the mass of catalyst introduced (also in grams), while x (%) is its weight content in titanium (atomic mass 47.9), one may write:

$$P_p = \text{advancement ratio}\,\frac{xP_c}{47.9 \times 10^{-3}}$$

because advancement ratio is generally expressed in terms of millimoles of titanium. Thus:

$$\text{advancement ratio} = \frac{P_p}{P_c}\,\frac{47.9 \times 10^{-3}}{x}$$

This equation holds for each particle within the polymer mass. For given supposedly spherical (catalyst or polymer) particle, one may write:

$$P_p = \tfrac{1}{6}\pi\rho_p d_p^3 \qquad P_c = \tfrac{1}{6}\pi\rho_c d_c^3$$

in which d_p, ρ_p, d_c, ρ_c are respectively the diameters and specific weights of polymer and catalyst. One thus obtains a theoretical law of the form:

$$\text{advancement ratio} = k_{th}(d_p^3/d_c^3) \quad (4)$$

with

$$k_{th} = \frac{\rho_p}{\rho_c}\,\frac{47.9 \times 10^{-3}}{x} \quad (5)$$

If one compares the theoretical equation (4) with the experimental relationship (3), one sees a perfect agreement as far as exponent 3 is concerned for d_p. Conversely, the slight disagreement as far as d_c exponent is concerned (2.8 instead of 3) may be explained on the basis of the lack of precision of measurements. Indeed the confidence interval of that exponent, at the probability threshold of 95% (i.e. $\pm 2\sigma$) is 2.82 ± 0.46.

For the third-generation catalysts examined in the present study, k_{th} (i.e. the theoretical value of k) was calculated from the known content (x%) in titanium and the specific weight ρ_c. Taking for polypropylene a value of $\rho_p = 0.9$ one obtains $k_{th} = 1.1$.

From *Figure 8*, the experimental value of k (first ordinate $= \log k$) is such that its logarithm may lie between -0.53 and $+0.67$ ($\log k \pm 2\sigma$); so k should lie between 0.29 and 4.68, and the most probable value is 1.17.

Comments about the relationship between advancement ratios and catalyst and polymer particle diameters

(i) A value for k_{th} may also be calculated, for a second-generation catalyst, from equation (5). Thus, from the known values of x (%titanium) and of the specific weight (ρ_c) of the catalyst used, in experimental series 1, and assuming the value 0.9 for the ρ_p of polypropylene, one obtains $k_{th} = 0.07$. This value, 16 times lower than the value obtained for third-generation catalysts, is in fair agreement with our experimental results, as discussed above. Indeed, if one calculates the K value for a third-generation catalyst having the same diameter as the experimental series no. 1 second-generation catalyst ($\bar{d} = 12.7\ \mu$m, *Table 2*), one obtains either $K = 8.93 \times 10^{-4}$ (from the regression line in *Figure 8*) or $K = 5.37 \times 10^{-4}$ (from the relationship $K = k_{th}/d_c^3$). These two values are respectively 20 and 12 times bigger than the K value for the second-generation catalyst, $K = 0.449 \times 10^{-4}$. The ratio between k and K values for the same catalyst diameter, in the cases of second- and third-generation catalysts, are of the same order of magnitude:

$$\frac{\text{third-generation catalyst } k \text{ value}}{\text{second-generation catalyst } k \text{ value}} = \frac{\text{third-generation catalyst } K \text{ value}}{\text{second-generation catalyst } K \text{ value}} = 16$$

(ii) Following the remarks in paragraph (i), one can say that relationship (4) is valid for third-generation catalysts, as well as for second-generation ones. Thus, there is an equivalent relationship between advancement ratios and catalyst and polymer diameters, irrespective of whether the polymerization was performed on supported or non-supported catalyst.

(iii) Relationship (3) was established for polymerization of propylene. It is valid for polymerization or copolymerization of other olefins, but with different values of k. Indeed, the derivation of that parameter involves the specific weight of polymer, which depends on the nature of the product.

(iv) Relationship (4) satisfactorily explains observed phenomena, for a wide range of advancement ratios. It is valid for the prepolymer range, as well as for polymers obtained from the most efficient catalyst on the current market.

Usefulness of the relationship between advancement ratios of polymers and catalyst and polymer diameters, in the industrial production of polyolefins

For a catalyst with a previously measured mean diameter, it is possible, through the use of relationship (4):

(i) to calculate, at any time during polymerization, the diameter of growing polymeric particles, from the amount of monomer consumed and the amount of catalyst introduced;

(ii) to determine minimum and maximum advancement ratios, in order to avoid, on the one hand, the presence of undesirably small particles (the so-called 'polymerization fines'), and, on the other hand, upsets of the stirring regime arising from the presence of undesirably large particles;

(iii) to fix values of the advancement ratio in order to obtain a prepolymer with a given diameter—the latter is especially useful in the case of a dry-phase fluidized-bed process, because too fine particles would be carried out of the polymerization zone as soon as they were introduced into the fluidizer.

Moreover, relationship (4) also allows the definition of the catalyst particle size to be used in order to obtain polymer particles of adequate diameter, taking into account the desired advancement ratio. Indeed, one

generally tries to obtain the highest possible yield in relation to the catalyst. That means a low level of catalytic residues and of catalyst cost per unit mass of polymer.

Finally, from an array of lines as shown by *Figure 5*, one can measure advancement ratio of polymer particles. A mere determination of the catalyst mean diameter, and of a polymer sample, leads to the advancement ratio value from the reading of the corresponding graph. In the special case of prepolymers with an advancement ratio lower than 20 g/mmol Ti the measurement method of the advancement ratio by chemical analysis (see above section) is relatively tedious and demands several hours. The method from mean diameter determination is much faster, since only 20 min are sufficient for a significant analysis of one sample. This method may thus be used as a control tool, in the context of industrial production.

CONCLUSIONS

Although automatic image analysis techniques have been used for many years in optical microscopy, the direct interfacing of image analysis on SEM does not seem to have led to a great deal of work so far. The present study is of main interest in illustrating the potential of the technique. In fact, although only low magnifications (of the order of some tens to some hundreds) have been considered at the moment, good reliability in dimension and shape measurements was demonstrated, even in the case of a shape somewhat remote from spherical symmetry.

Within about 20 min, on a previously well prepared sample, significant measurements may be performed, using ~ 150 particles (5–6 microscope fields). This is true for polymer particles as well as for starting catalyst particles, provided that the latter are dispersed on a sample holder and subsequently transferred under an inert dry atmosphere. It thus seems feasible to use the method as such with a medium-quality, relatively cheap SEM, within an industrial environment (control laboratory).

Because of the value of results obtained on catalysts, it was possible to demonstrate, for the case of third-generation catalysts (supported catalysts), which show a 'superactivity' in olefinic polymerization, the growth laws previously demonstrated in the case of second-generation catalysts (non-supported ones). The only point not thoroughly examined, but which could now be easily considered, is the representativeness of sampling, i.e. the true dispersion of the various particles, especially catalyst ones.

By using much greater magnifications in SEM, it should be possible to perform a quantitative morphological study on a single particle. One could thus examine whether the replication observed between starting catalyst particles and resulting polymer grains (for every advancement ratio) is also present down to the microporous structure level.

With the same methods as used above, one can count and measure individual microvoids seen within one particle, as one did for the grains themselves.

We therefore believe that this automatic image analysis technique, interfaced with SEM, will develop in the near future, for studies on catalyst and corresponding polymer particles.

ACKNOWLEDGEMENTS

The authors wish to thank BP Chemicals' Catalyst Research Group for sampling work and staff at Institut Textile de France for carrying out morphological and analytical work.

REFERENCES

1 Boor, J. (Shell Development Co.) 'Ziegler–Natta Catalysts and Polymerization', Academic Press, New York, 1979, Ch. 8, pp. 180–212
2 'Particle Size Measurement', *J. GAMS*, Ecole Polytechnique de Palaiseau, France, 27–28 Oct. 1982
3 'Particle Size Analysis', R. Soc. Chem. Conf. (Analytical Division), University of Bradford, UK, 16–19 Sept. 1985
4 Coultronics France Ltd, 14 Rue E. Legendre, Margenay, 95580 Andilly, France
5 Guichard, 'Un appareil de mesure granulométrique; le compteur automatique Coulter', *Chim. Anal.* 1965, **3**, 145–151
6 Apparatus marketed by 'Instrumat', Av. des Andes, Z.A. de Courtaboeuf, BP 86, 91943 Les Ulis, France
7 'Optomax' (Image Analyzer), 'Micromeasurements Ltd', Shirehill Industrial Estate, Shirehill, Saffron Walden, Essex CB11 3AQ, UK
8 'Microconsultants' Group, Kenley House, Kenley Lane, Kenley, Surrey, CR2 5YR, UK
9 Hagege, R., Delmas, J. L., Thiroine, C. and Raye, I. *Bull. Sci. ITF—15*, 1986, **60**, 41–61
10 'Imaging Technology Inc.', Technical Publ. Dept, 600 West Cumming Park, Woburn, MA 01801, USA
11 'Noesis' Ltd, Z.A. Les Metz, 78350 Jouy en Josas, France
12 Fr. Pat. 2340131 (Naphtachimie), 1976, 2, 3
13 Fr. Pat. 2381565 (Naphtachimie), 1977, 2, 23
14 Fr. Pat. 2596052 (BP Chimie), 1986, 3, 20
15 Eur. Pat. 98196 (BP Chimie), 1983, 6, 14
16 Eur. Pat. 99284 (BP Chimie), 1983, 6, 14
17 Eur. Pat. 99773 (BP Chimie), 1983, 6, 14
18 Technical sheet 'Titanium trichloride catalysts and intermediates —Products Data' (Stauffer Chemical Co., Speciality Chemical Division, Westport, Connecticut; Toyo Stauffer Chemical Co., Tekkosha Bldg, 3-2-4 Kyobashi, Chuo-Ku, Tokyo; Toho Titanium Co., 3 Aoi-Cho, Minato-Ku, Tokyo)
19 Triplett (Stauffer Ltd) *Appl. Ind. Catal.* 1983, **1**, 177–205
20 Karol (Union Carbide Ltd), *Catal. Rev. Sci. Eng.* 1984, **23**(3), 557–95
21 Galli, *Angew. Makromol. Chem.* 1981, **94**, 63–89
22 Galli, 5th Rubber Europ. Conf., Paris, 1978, vol A5, pp. 1–7
23 Intern. Conf. 'Europlastics', Paris, April 1988